Stratification of Metal and Sulphate Loads in Acid Mine Drainage Receiving Water Dams – Variables Regionalization by Cluster Analysis

J.A. Grande*[1], M.L. de la Torre[1], T. Valente[1,2], J.P. Fernández[3], J. Borrego[1], M. Santisteban[1], J.C. Cerón[1], D. Sánchez-Rodas[4]

ABSTRACT: The Sancho Reservoir (Iberian Pyrite Belt, SW Spain) is nourished by the waters of the river Meca, which is affected by acid mine drainage (AMD) processes from the abandoned Tharsis mine. The aim of the present work is to study the hydrochemical variations in this reservoir, in order to define potential stratification processes in metal load and sulphates. A stratified sampling from the surface, with one meter deep intervals to the bottom of the dam, was performed. The results show a clear stratification of temperature, pH, electric conductivity, dissolved oxygen, metal and sulphate loads associated with depth. There is an increase of metal loads at the bottom of the reservoir, though previous studies only detect iron. The proximity between pH and aluminium suggests that water chemistry is strongly influenced by aluminium precipitation processes. This indicates the buffer effect that aluminium exercises, which precipitates as amorphous or low crystalline phases, introducing hydrogen ions to the system, while alkalinity input tends to raise pH. *Water Environ. Res.*, **87,** 626 (2015).

KEYWORDS: AMD, dam, cluster analysis, hydrochemical zonation, Iberian Pyrite Belt.

doi:10.2175/106143015X14212658614793

Introduction

The studied area is located in the Iberian Pyrite Belt, in the southwest of Spain (Figure 1). It contains numerous, giant and super giant Palaeozoic massive sulphide deposits, the largest in the world according to Sáez et al. (1999). These authors place the reserves above 1500 m distributed in eight super giant deposits (>100 m) and a non precise number of other smaller deposits, commonly associated with stockwork mineralizations and footwall alteration haloes. The massive sulphide bodies contain pyrite, with which sphalerite, chalcopyrite and many minor phases are associated (Sáez et al., 1999). These deposits have been exploited for more than 2000 years. Today, numerous remains of this activity persist, such as extensive mining works and million of tons of former slag with varied composition (Pinedo Vara, 1963 in Grande et al., 2005a). This generated a particularly degraded scenario, with more than 500 ha affected by mining activity. There are all kinds of mining structures, which were not restored despite activity closure and that, therefore, continue to release leached acid to the river network.

Acid Mine Drainage (AMD) is one of the most serious types of water contamination due to its nature, magnitude, difficult solution and remediation costs (Azcue, 1999; Commonwealth of Pennsylvania, 1994). The affected streams are characterized by water acidity, high metals and sulphate levels, as well as by metallic contamination of associated sediments.

The damage caused on ecosystems can range from sub-lethal effects, such as in low contamination levels related to bioaccumulation and biomagnification (Nebel et al., 1999), to severe changes which cause riverine biodiversity disappearance and make water resources useless for human, agricultural or industrial uses (Sáinz. 1999).

This type of contamination occurs when a sulphide ore contacts with oxygen and atmospheric moisture (Sáinz, 1999); a complex mechanism begins on the mineral surface that starts with sulphide oxidation, leading to acid production and sulphates. The kinetics of this oxidation reaction are very slow, between $1{,}08\times10^{-1}$ to $1{,}8.10^{-1}$ mol/(cm^2.s) and can be increased 100 times by the presence of ferric ions (Dogan, 1999) and by bacteria catalytic action (Nicholson, 1994). Other secondary processes occur (Förstner et al., 1998), and the final result is a set of soluble contaminants deposited on the mineral, which are then dissolved and washed away by rainwater or runoff, promoting contamination of water courses. Though the sulphide oxidation phenomenon is a natural fact, production rates caused by mining can be distinguished from the natural geochemical process (acid rock drainage or ARD) and the anthropogenic process caused by the surfaced mineral massive amount and by the increase of contact surfaces due to mining (AMD) (EMCBC 1996).

The AMD and ARD processes that affect the regional drainage network have been extensively described by several authors (Aroba et al., 2007; Borrego, 1992: Borrego et al., 2002; Borrego et al., 2011; Carro et al., 2011; Braungardt et al., 1998; Davis et al., 2000; de la Torre et al., 2009; de la Torre et al., 2010; de la Torre et al., 2011; Elbaz-Poulichet et al., 1999; Elbaz-Poulichet et al., 2000; Elbaz-Poulichet et al., 2001; Grande, 2011;

[1*] Centro de Investigación para la Ingeniería en Minería Sostenible. Escuela Técnica Superior de Ingeniería. Universidad de Huelva. Ctra. Palos de la Frontera. s/n. 21819. Palos de la Frontera. Huelva. Spain; email: grangil@uhu.es

[2] Centro de Investigação Geológica, Ordenamento e Valorização de Recursos, Departamento de Ciências da Terra, Universidade do Minho, Campus de Gualtar, 4710-057 Braga. Portugal.

[3] Departamento de Explotación y Prospección de Minas. Universidad de Oviedo. Escuela Politécnica de Mieres.c/ Gonzalo Gutiérrez Quirós, s/n. 33600. Mieres. Spain.

[4] Grupo de Geoquímica Ambiental. Facultad de Ciencias Experimentales. Universidad de Huelva. 21071. Huelva. Spain.

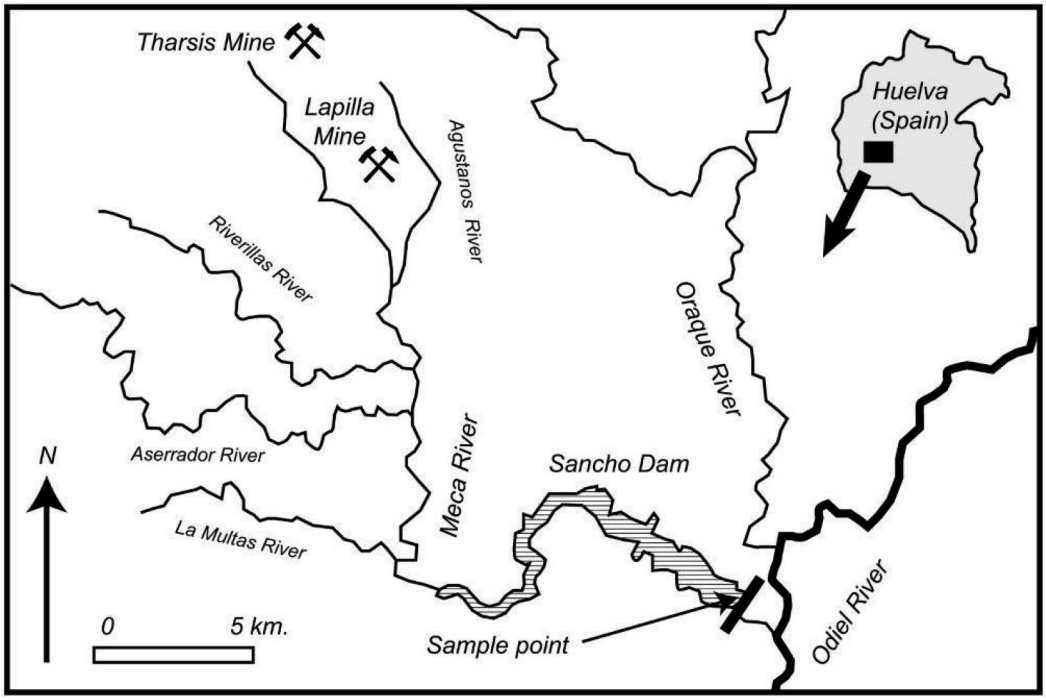

Figure 1—Location map.

Grande et al., 2000; Grande et al. 2003a; Grande et al., 2003b; Grande et al., 2005a; Grande et al., 2005b; Grande et al., 2007; Grande et al., 2009; Grande et al., 2010a; Grande et al., 2010b; Grande et al., 2010c; Grande et al., 2010d; Grande et al., 2010e; Grande et al., 2011a; Grande et al., 2011b; Jiménez et al., 2009; Leblanc et al., 2000; Sáinz et al., 2002; Sáinz et al., 2003a; Sáinz et al., 2003b; Sáinz et al., 2004; Sáinz et al., 2005).

In semi-arid climates, dam construction is one of the most common alternatives to cover population and industry water needs. The vulnerability of these water surfaces against contamination is much greater than in underground waters (Grande et al., 2010d). The Sancho Dam was built in 1962 and is nourished by the waters of the river Meca (Figure 1). It has a maximum storage capacity of 58 Hm^3 and the impounded water covers an area of 427 ha. The total watershed area is of 314 km^2 with a crest length of 224 m and 56 m height above sea level.

River Meca (Figure 1) receives contaminated waters from different subsidiary tributaries affected by AMD processes mostly from the abandoned Tharsis mine (SW Spain). Here, waste-dumps occupy an area of more than 300 ha. In addition, there are two big open pits and endless mining facilities, which give a scenario particularly degraded by industrial activity, responsible for AMD generation. The dam water is used for industrial purposes to supply the pulp mill located 15 km downstream, in San Juan del Puerto (SW Spain).

Several authors have described the processes which affect Sancho water dam: Sarmiento et al., (2009) describe natural attenuation processes, while Torres et al., (2010) make a proposal for the dam geochemistry control process. Using a more detailed sampling network, the present work aims to study the hydrochemical variations in Sancho water dam, in order to define potential stratification processes in metal charge and sulphates.

Geological Setting. The stratigraphic regional series of Iberian Pyrite Belt (IPB) (Figure 2) reveals a highly complex lithology with many different types of rocks which have great variation in their spatial and temporal distribution. It is characterized by abundant wedging, lenses, changes in thickness and transit between different types of rock, which are especially revealed in the intermediate unit, known as the volcano-sedimentary complex (VSC). Right in the transition from the Devonic to the Carboniferous, a large homogeneous marine basin with a gently undulate topography and shallow platform has broken and collapsed. The original platform led to a steep set of subbasins with different subsidence rates and slope stability, where different kinds of rocks have accumulated. In some of them sulphides were deposited and a sufficient quantity was preserved to form deposits. This happened simultaneously when magmatism and variscan tectonic activity increased in intensity. The maximum phase of tectonic deformation took place during the Late Carboniferous (Westphalian), matching in time with the last Culm group deposits (Moreno and González, 2004). Essentially, there are three major units, which are described below due to potential influence of respective lithology on the water dam chemistry.

Devonian Pre-Volcanic Sediments (PQ group). PQ lithostratigraphic features are the same throughout the whole IPB, except near the top where some differentiation is observed in different places. Most of the stratigraphic column unit consists of dark shales (gray to black) with fine sandstone layers. These facies represent deposition in a shallow marine environment (McGillavry, 1961), which is a low energy shallow marine platform, rarely submitted to storm action (Moreno and Sáez 1990; Sáez and Moreno 1997).

Volcano-Sedimentary Complex (VSC). VSC corresponds to the time when magmatic activity (effusive and subvolcanic)

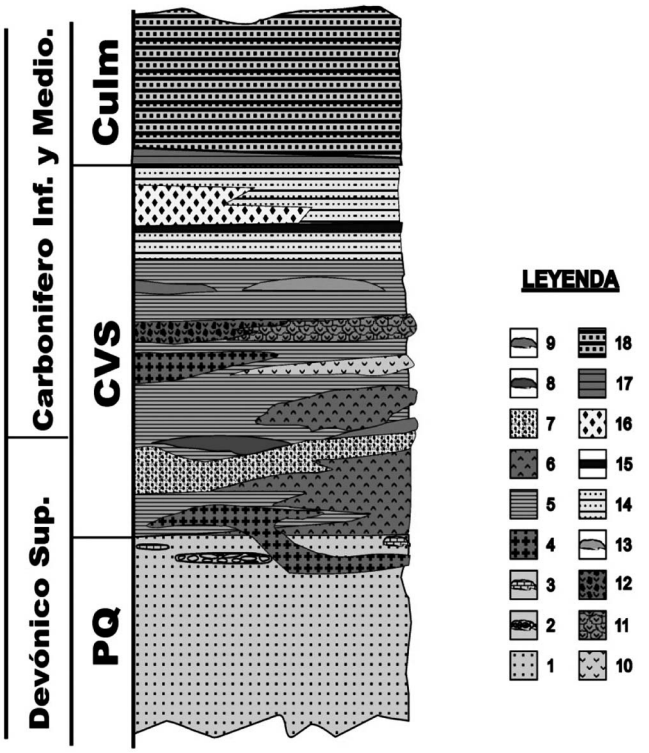

Figure 2—Stratigraphic column of Iberian Pyrite Belt. 1) Shales and quartzites of PQ Group, 2) Conglomerates and litharenites, 3) Fossiliferous limestones, 4) Basic subvolcanic rocks, 5) Black and gray shales, locally siliceous, 6) Felsic rocks (rhyolites and dacites), 7) Felsic vulcanoclastic rocks, 8) Massive sulphides, 9) Mn jaspas, 10) Mafic coherent rocks (lavas), 11) Pillow lavas, 12) Lavas, breccias and tuffs, 13) Green and gray chert, 14) Vulcanoclastic rocks with varied grain size, 15) Purple shales, 16) Vulcanoclastic coarse-grained rocks, 17) Shales and fine-grained vulcanoclastic rocks, 18) Shales and litharenites of Culm Group, (Moreno et al., 1996; Moreno and González, 2004).

conditioned geological processes. This unit includes massive sulphide mineralization and manganese. Its age has been established between Faminiense (Estruniense) and Namuriense peak, based on palynomorphs (Moreno et al., 2003; Lake, 1991).

From a lithological point of view, VSC consists of a heterogeneous sedimentary series with interbedded magmatic rocks of different nature and composition. Among sedimentary rocks, those of detrital and vulcanoclastic origin predominate. The last ones result from erosion and re-deposit of non-cohesive volcanics. One should also notice the common presence of chemical sedimentary rocks, which should include massive sulphides, manganese jaspers and some discontinuous levels of fossiliferous limestones. Shaly lithofacies are composed by shales and dark colored siltstones and variable organic matter content (Sánchez-España et al., 2000; Yusta et al., 2002; Tornos et al., 2008; Sáez et al., 2010). At the VSC top appears an oxidized sequence of red/ violet colours between clay and sand size. Usually, its thickness does not exceed 10 m and very rarely can come to 100 m. On the other hand, its lateral continuity is very large and has probably covered most of the IPB by the time of its deposit, in a continuous way.

Culm Group. The Culm group is the youngest stratigraphic unit of IPB. It represents the infill of a subsiding basin by turbidite sediments (Oliveira, 1983), whose source areas would be both the IPB and eroding northern units, including the Ossa-Morena Zone of the Iberian Massif (Moreno, 1993; Sáez et al., 1999). It comprises the sedimentary and postvulcanic rocks of IPB. Petrographic studies reveal that fragments of sedimentary and volcanic origin are the major lithic components of the Culm litharenites. This, together with other sedimentological and paleogeographic data suggests that part of IPB was submitted to erosion and therefore emerged (Moreno, 1993; Moreno and González, 2004).

Materials and Methods

This study aims to define the vertical hydrochemical variations in the Sancho water reservoir and the establishment of potential vertical and horizontal stratification processes, concerning metal and sulphates loads. For this, a stratified sampling at the base of the dam wall, from the surface with one-meter deep intervals to the bottom of the reservoir, was performed in October 2011.

Table 1—Summary statistics of analyzed parameters.

Parameter	Average	Variance	Standard deviation	Coefficient of variation %	Minimum	Maximum	Rank
pH	3.9	0.2303	0.4802	12.23	3.5	4.6	1.17
Cond. (μS/cm)	441.57	279.21	16.71	3.78	401	472	71
T (°C)	22.37	20.09	4.48	20.03	14.6	25.8	11.2
TSD (mg/L)	283.03	115.81	10.76	3.80	257	302	45
OD (mg/L)	3.79	5.5108	2.34	69.08	0.16	6.16	6
Fe (mg/L)	0.75	0.0250	0.15	20.96	0.54	1.16	0.62
Al (mg/L)	0.01	0.0029	0.05	54.82	0.012	0.20	0.19
Cd (mg/L)	0.13	0.000	0.01	7.27	0.108	0.147	0.039
Cu (mg/L)	0.63	0.0076	0.08	13.73	0.418	0.807	0.389
Mn (mg/L)	1.48	0.0140	0.12	7.99	1.08	1.68	0.589
Ni (mg/L)	0.01	6.609 E-8	0.0002	2.49	0.009	0.01	0.001
Pb (mg/L)	1.02	0.13	0.35	34.66	0.27	1.91	1.63
Sb (mg/L)	0.002	5.196 E-7	0.0007	31.98	0.0012	0.0034	0.0022
Zn (mg/L)	2.27	0.1288	0.35	15.78	1.49	2.73	1.23
SO_4^{2-} (mg/L)	181.75	91.23	9.55	5.25	170	199	29

A Hydro-bioss sampler bottle (Kiel-Altenholz, Germany) was used to extract samples at different depths, which allows defining precisely the vertical variations for each pollutant.

The temperature, pH, conductivity and total dissolved solids were measured *in situ* using a portable multiparametric CrisonMM40 (EE.UU). Dissolved oxygen was measured with a HydrolabQuanta (EE.UU) probe.

Contrary to previous studies (Sarmiento et al., 2009; Torres et al., 2010), which were based only in three sampling points, the present work allowed to obtain a total of 28 samples, at one-meter intervals. Double samples were taken and nitric acid was added to one of them, to prevent metals precipitation. Sulphate content was determined in the no acidified sample. Metals concentration was determined using atomic absorption spectrophotometry, while sulphates were determined by photometry.

Statistical treatment was performed using the Statgraphic Centurion (EE.UU) package, to obtain a statistical summary, depth graphics evolution and clustering analysis dendrograms.

Results

Table 1 presents the variables statistical summary. The study found that pH values range from 3.5 in the most superficial part, increasing with depth to 4.6 with a 3.9 average value for the whole water column. This range of values shows an obvious effect of AMD processes in the watershed. Average metals and sulphates concentrations are highly affected by dilution processes in the reservoir and, therefore, are far below the expected values in a mining reservoir or in an AMD channel, as it was already described by several authors (e.g. Grande et al 2003a & 2005a; Valente & Leal Gomes, 2009).

Concerning depth evolution, the study found that temperature (T) stays mostly stable around 26 °C to 16 m, showing a decrease tendency to 20 m. From this point on, the decrease becomes less pronounced (Figure 3). A similar pattern was found for pH, with stable values around pH 3.5 to 16 m, from where a sharp rise is produced to 20 m; when reaching values close to 4.6 this parameter tends to stabilize.

Something very similar happens to dissolved Oxygen (DO), presenting high values between 5 and 6 mg/L, with a slow decrease in the first 15 m. At this point, a strong decrease to 19 m occurs. Here, values close to zero are shown. The three described variables show a transition zone between 15 and 20 m. Conductivity and TDS have nearly an identical plot with smooth decreases to 15 m and an abrupt decrease to 20 m. At this point there is a new development, concerning an increase with depth. Sulphates (SO_4) develop in a similar way to the previous variables with a minimum concentration around 5 m.

The fitness function (4-order polynomial) shows clearly the development of each variable with depth. The variables copper (Cu), iron (Fe), conductivity, TDS, manganese (Mn), and cadmium (Cd) show decreasing values with depth to 15 m and from this point on they show increasing trends (Figure 3). The variables dissolved oxygen (DO), nickel (Ni), antimony (Sb), temperature (T), and zinc (Zn) show smooth decreasing values to 15 m. At this point a sudden drop to 20 m is produced in all of them, and from now on values stay constant or in a slow decline (Figure 3). pH stays stable to 15 m from where a sudden rise occurs to 20 m and tends to stabilize when reaching 4.6 close values. Lead (Pb) and aluminium (Al) show rising values in depth along the whole water column. Sulphates show a different behaviour, somehow similar to TDS and conductivity, but with a unique increase at 15 meters.

Regarding cluster analysis, using Euclidean Ward's method (Figure 4) clearly shows two family groups: the variables T, DO, Zn, Sb, Ni and SO_4 group and the remaining variables group. In this graph, it is striking that pH is only closely related to Al and in a more discreet way with depth and Fe. It is placed very far from the rest of the variables. On the other hand, conductivity and TDS are very close with each other and not far from Cd, Cu and Mn. The variable DO is close to zinc and to temperature.

Cluster analysis of sampling sites (Figure 5) according to euclidean quadratic distance method clearly groups the variables in 3 classes corresponding to depths: (0–16 m), (16–20 m) and (20–28 m).

Discussion

In temperate regions water reservoirs tend to be strongly stratified in summer. The warmer upper part (epilimnion) isolates itself from the colder one (hypolimnion) in an area called the thermocline that acts as a barrier for exchange materials. This soon causes insufficient supply of oxygen in the hypolimnion and of nutrients in the epilimnion. By fall, the upper layer cools down and wind effect mixes water. Water mixing may produce phytoplankton blooms because water circulation brings nutrients to the surface. One should remember that in this study sampling was performed in late summer.

In the present case, the water chemistry was conditioned by sulphide oxidation processes. Sulphides oxidation reactions, as described by Nordstrom et al. (1999), cause an increase of dissolved solids and a pH decrease. In the presence of oxygen, Fe^{2+} mobilized from iron sulphide oxidizes to Fe^{3+}. In general, as long as pH does not reach 3, the ferric ion precipitates as oxyhydroxisulphate, promoting its decrease in solution, while pH drops by liberating hydrogen ions (López-Pamo et al. 2009; Santofimia et al., 2012). According to these authors, for pH close to 3, Fe^{3+} concentration increases and acts as pyrite oxidant without the need of dissolved oxygen, giving to the system more Fe^{2+}, SO_4^{2-} and H^+.

Acidity from AMD may cause aluminosilicates dissolution from host lithologies (e.g. Younger, 2002). This process consumes hydrogen ions and brings to water dissolved elements such as Al, Mg, Fe^{2+} and others. The same was observed by other authors (López-Pamo et al., 2009), that demonstrate that chlorite dissolution coming from host slates, in different IPB acidic mine pit lakes, brings to solution significant amounts of Fe^{2+} and Mg (Vasquez et al., 2011). Acidity consumed in the dissolution process is less than potential acidity related to Fe release.

Depth evolution graphs (Figure 3) and cluster dendrogram (Figure 5) show a clear stratification of T values, pH, conductivity and dissolved oxygen, as well as the corresponding metal and sulphate loads associated with depth. This scenario is similar to the one described by Doyle and Runnells (1997) in López-Pamo et al. (2009), showing a more dense lower layer (monimolimnion) which is located between 20 m and 28 m and does not mix with the rest. There is also a superficial layer (epilimnion), located between 0 m and 16 m and submitted to evaporation and circulation, as well as a mixed layer located

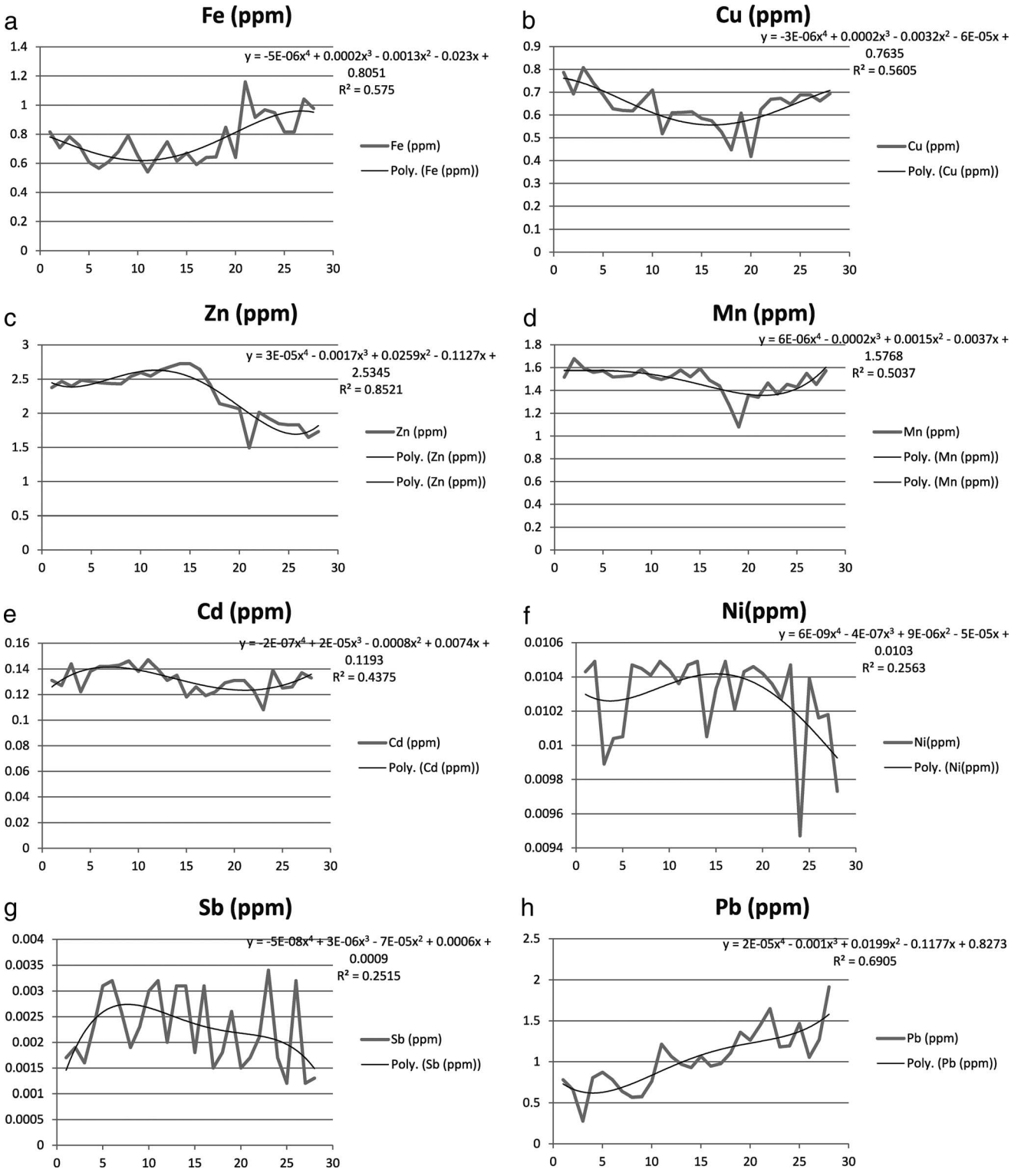

Figure 3—Depth evolution of parameters with fitness function (4-order polynomial).

between the previous ones (mixolimnion), which should be located between 16 m and 20 m.

The dendrogram of Figure 4 shows clearly the proximity of pH and aluminium, and, therefore, suggests that this water chemistry is strongly influenced by aluminium precipitation processes. This reservoir seems regulated by aluminium precipitation, as described by López-Pamo et al. (2009). The statistical summary data (Table 1) indicates how small pH variations (from 3.5 to 4.6) strongly influence vertical aluminium concentrations (from 0.01 ppm to 0.2 ppm). This indicates the

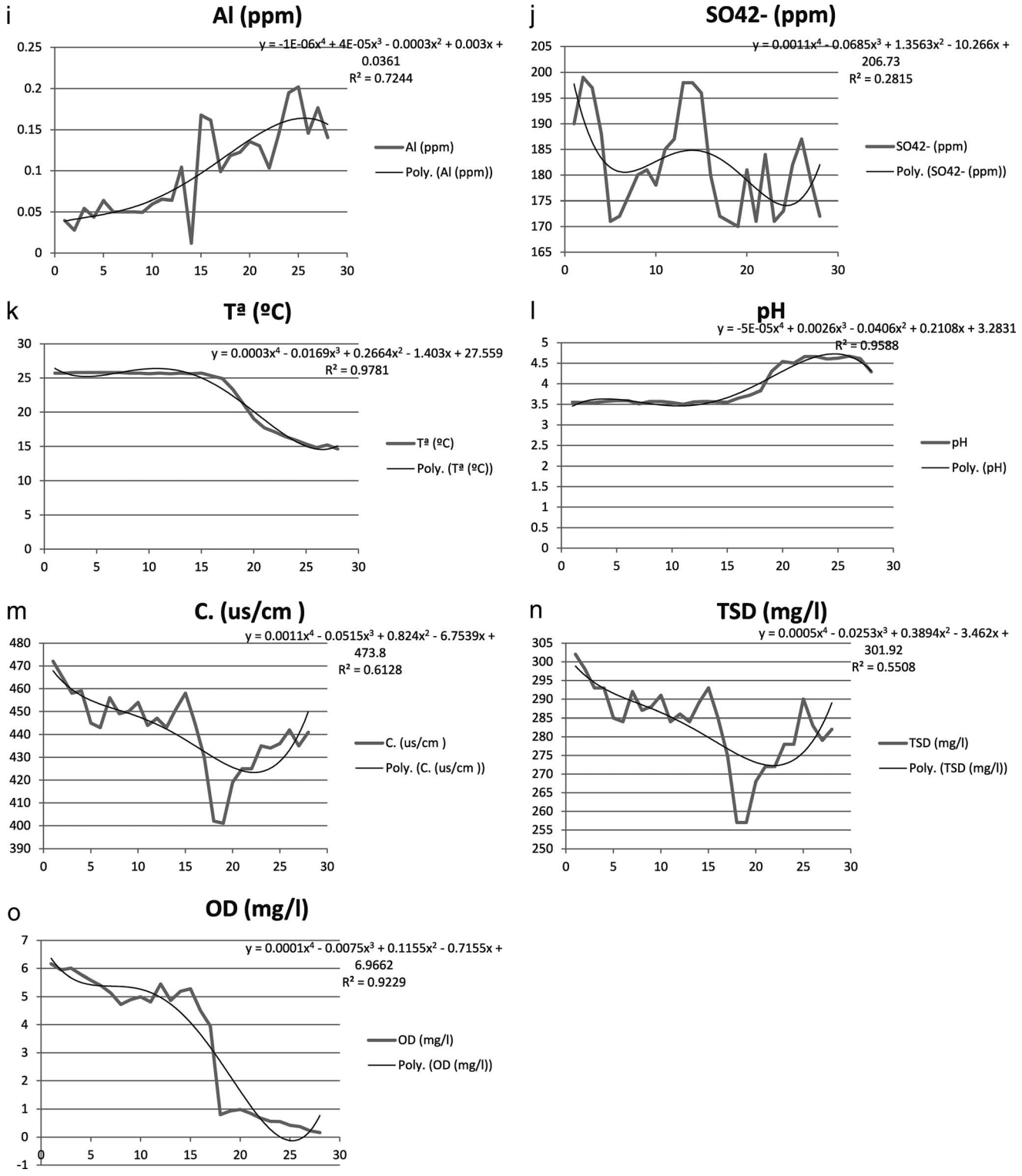

Figure 3—(Continued)

buffer effect that aluminium exercises, which precipitates as amorphous or low crystalline phases, introducing hydrogen ions to the system, while alkalinity input tends to raise pH.

Concerning the parameters pH, temperature and dissolved oxygen, it should be emphasized that behaviours match with the ones described by Torres et al. (2010) for the late summer period, when hydrochemical stratification happens. In fact, the values found in the present study for deep layers are close to the ones mentioned by these authors. Regarding conductivity, the results are clearly different from those of Torres et al. (2010) and

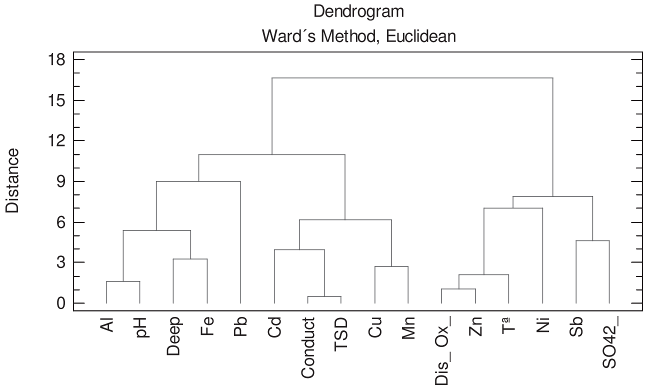

Figure 4—Cluster analysis of variables.

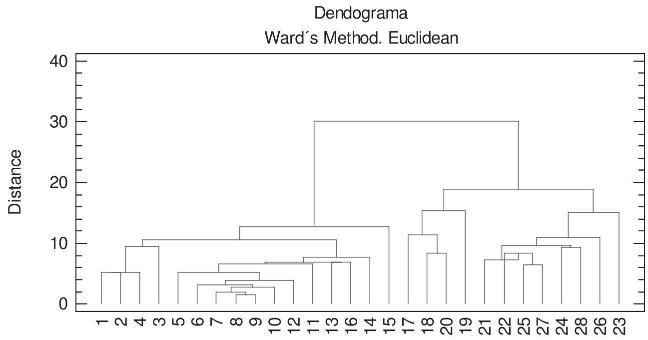

Figure 5—Cluster analysis of observations.

quite similar to those described by Sarmiento et al. (2009), though for these authors there is no significant tendency. In the present study a much clearer tendency is seen, with minimum values in the hypolimnion at 20 m and an increase to 28 m. This phenomenon is important to justify the metal load increase in the hypolimnion.

Concerning dissolved metal loads some similarities and differences with the previously mentioned studies may be pointed out. In matters of pollutants, As wasn't found and similar values of iron, copper, zinc, nickel and antimony were found. In relation to copper, the present values range between 0.4 and 0.8 ppm, identical to the ones proposed by ENCE, the dam operating company (internal information from monthly sampling). This range is also similar to the one found by Sarmiento et al. (2008), but very different from the one proposed by Torres et al (2010). Regarding iron, it ranges from 0.5 ppm to 1.2 ppm, almost identical values to those found by Sarmiento et al (2009) and clearly different from those of Torres et al. (2010), which reach a maximum of 4.2 ppm.

For zinc, the values obtained in the present study are identical to those of referenced works. Nickel and antimony have similar values, in the range of ppb, though somehow lower than those proposed by Sarmiento et al. (2009). The most significant differences are found in aluminium, which in the present study assumes values 26 times lower than those found by Torres et al. (2010). Something similar happens with manganese concentration, which for this study is much lower than the one described in the referenced studies. It is important to note that atomic absorption data was compared using ICP (Inductively Coupled Plasma) and no significant differences were found. Equally, the present data was compared with the ones from ENCE, which perform monthly sampling, obtaining identical results.

Another substantial difference is the one found for lead and cadmium. In this case, values are clearly higher, about 300 times more in the case of lead; 1.9 ppm maximum and only 6 ppm for Torres et al. (2010). Similar difference was found for cadmium.

Increasing concentrations in the hypolimnion is more evident for copper, lead, iron, aluminium and manganese. In the cases of cadmium, nickel and antimony, coming to ppb levels, variations are smaller. The only metal that does not follow this tendency is zinc.

This metal increase in the hypolimnion is followed by sulphate concentration decrease, comparing with the epilimnion. Unlike other records, the obtained data put in evidence the increase of metal load at the bottom of the reservoir, though previous studies only detect it for iron.

pH increase that occurs in the hypolimnion is well described by Torres et al. (2010), justifying the phenomenon based on the highly reducing conditions that characterize this zone. These conditions cause reduction and redissolution of iron(III) that may be present in the form of schwertmannite, which would explain iron and pH increase through the reaction:

$$Fe_8O_8(OH)_{5.5}(SO4)_{1.25} + 13.5H^+ + 2CH_2O ------8Fe^{2+} + CO_2(aq) + 1.25\,SO4^{2-} + 11.5H_2O$$

This dissolution process should be followed by mobilization of other metals that are adsorbed to the iron precipitate. Decreasing sulphate near the bottom may be explained by microbiological reduction, in accordance with the following reaction that also consumes hydrogen ions, promoting pH increase:

$$SO_4^{2-} + 2CH_2O + 2H^+ ------------------------------ CO_2(aq) + H_2S + 2H_2O$$

In addition to sulphate reduction, several authors described reduction of metallic compounds by organic matter (Wetzel, 2001; Schlesinger, 2005; Boehrer and Schultze, 2008). This process may also explain the metals increase in the hypolimnion, near the bottom, through the reactions:

$$2\,MnO_2 + 2CH_2O + 4H^+ ------------------------------ 2\,Mn^{2+}CO_2 + H_2O$$

$$4\,Fe(OH)_3 + CH_2O + 8H^+ ------------------------------ Fe^{2+}CO_2 + 11\,H_2O$$

This possibility is supported by the behaviour of conductivity and total dissolved solids, which presented similar trends to the ones observed for metals.

Conclusions

Depth evolution graphs and cluster dendrogram show a clear stratification of Temperature, pH, electric conductivity and dissolved oxygen, as well as the corresponding metal and sulphate loads associated with depth in the Sancho reservoir. Unlike other records, the obtained data provide evidence of the increase in metal load at the bottom of the reservoir, though previous studies

only detect it for iron. Concentrations of copper, lead, iron, aluminium, and manganese increased in the hypolimnion. In the cases of cadmium, nickel, and antimony, concentrations in the hypolimnion were lower (ppb levels), and variations smaller. The only metal that does not follow this tendency is zinc.

This metal increase in the hypolimnion is followed by sulphate concentration decrease, compared with the epilimnion. Decreasing sulphate near the bottom may be explained by microbiological reduction, which consumes hydrogen ions, promoting pH increase.

The dendrogram shows clearly the proximity of pH and aluminium, and therefore suggests that this water chemistry is strongly influenced by aluminium precipitation processes. This indicates the buffer effect that aluminium exercises, which precipitates as amorphous or low crystalline phases, introducing hydrogen ions to the system, while alkalinity input tends to raise pH.

Acknowledgements

Financial support for this research was provided by DGCICYT National Plan, project CGL2010-21268-C02-01.

Submitted for publication February 5, 2013; accepted for publication August 30, 2013.

References

Aroba, J.; Grande, J. A.; Andújar, J. M.; de la Torre, M. L. (2007) Application of Fuzzy Logic and Data Mining Techniques as Tools for Qualitative Interpretation of Acid Mine Drainage Processes. *Environ. Geol.*, **53**(1), 135–145.

Azcue, J. M. (1999) *Environmental Impacts of Mining Activities*; Springer: Heidelberg, Germany.

Boehrer, B.; Schultze, M. (2008) Stratification of lakes. *Rev. Geophys.*, **46** (2) RG2005.

Borrego, J. (1992) *Sedimentología del estuario del Río Odiel, Huelva, S.O. España*. PhD Thesis. University of Sevilla

Borrego, J.; Morales, J. A.; de la Torre, M. L.; Grande, J. A. (2002) Geochemical Characteristics of Heavy Metal Pollution in Surface Sediments of the Tinto and Odiel River Estuary (Southwestern Spain). *Environ. Geol.*, **41,** 785–796.

Borrego, J.; Carro, B.; López-González, N.; de la Rosa, J.; Grande, J. A.; Gómez, T.; de la Torre, M. L. (2011) Effect of Acid Mine Drainage on Dissolved Rare Earth Elements Geochemistry Along a Fluvial-Estuarine System: the Tinto-Odiel Estuary (SW Spain). *Hydrology Research*. **43**(3), 262–274.

Braungardt, C. B.; Achterberg, E. P.; Nimmo, M. (1998) Behaviour of Dissolved Trace Metals in the Rio Tinto/Río Odiel Estuarine System. In *European Land-Ocean Interaction Studies*, Second Annual ELOISE Scientific Conference, Huelva, Spain, September 30-October 3;Morales, J.A.; Borrego, J. Eds; Abstract 51.

Carro, B.; López-González, N.; Grande, J. A.; Gómez, T.; Valente, T. (2011) Impact of Acid Mine Drainage on the Hydrochemical Characteristics of the Tinto-Odiel Estuary (SW Spain). *J. Iberian Geol.*, **37**(1), 87- 96.

Commonwealth of Pennsylvania. (1994) *Water Quality Assessment in Western Pennsylvania Watershed*; Commonwealth of Pennsylvania. Department of Environmental Protection: Pennsylvania. USA.

Davis, R. A. Jr.; Welty, A. T.; Borrego, J.; Morales, J. A.; Pendón, J. G.; Ryan, J. G. (2000) Rio Tinto Estuary (Spain): 5000 Years of Pollution. *Environ. Geol.*, **39,** 1107–1116.

de la Torre, M. L.; Grande, J. A.; Jiménez, A.; Borrego, J.; Díaz Curiel, J. M. (2009) Time Evolution of an AMD-Affected River Chemical Makeup. *Water Resour. Manage.*, **23**(7), 1275–1289.

de la Torre, M. L.; Sánchez-Rodas, D.; Grande, J. A.; Gómez, T. (2010) Relationships Between pH, Color and Heavy Metal Concentrations in the Tinto and Odiel Rivers (Southwest Spain). *Hydrol. Res.*, **41**(5), 406–413.

de la Torre, M. L.; Grande, J. A.; Graiño, J.; Gómez, T.; Cerón, J. C. (2011) Characterization of AMD Pollution in the River Tinto (SW Spain) Geochemical Comparison Between Generating Source and Receiving Environment. *Water, Air, Soil Pollut.*, **216,** 3–19.

Dogan, P. A., (1999) Characterization of Mine Waste for Prediction of Acid Mine Drainage. In *Environmental Impacts of Mining Activities*; Azcue, J.M. Ed.; Springer: Berlin, pp. 19–38

Doyle, G. A.; Runnells, D. D. (1997) Physical Limnology of Existing Mine Pit Lakes. *Mining Engineering*, **49,** 76–80.

Elbaz-Poulichet, F.; Morley, N. H.; Cruzado, A.; Velasquez, Z.; Achterberg, E. P.; Braungardt, C. B. (1999) Trace Metal and Nutrient Distribution in an Extremely Low pH (2.5) River-Estuarine System, the Ria of Huelva (South-West Spain). *Sci. Total Environ.*, **227,** 73–83.

Elbaz-Poulichet, F.; Dupuy, C.; Cruzado, A.; Velasquez, Z.; Achterberg, E.; Braungardt, C. (2000) Influence of Sorption Processes by Iron Oxides and Algae Fixation on Arsenic and Phosphate Cycle in an Acidic Estuary (Tinto river, Spain). *Water Res.*, **34**(12–15): 3222–3230.

Elbaz-Poulichet. F.; Braungardt, C.; Achterberg, E.; Morley, N.; Cossa, D.; Beckers, J.; Nomérange, P.; Cruzado, A.; Leblanc, M. (2001) Metal Biogeochemistry in the Tinto-Odiel rivers (Southern Spain) and in the Gulf of Cadiz: A Synthesis of the Results of TOROS Project. *Cont. Shelf Res.*, **21**(18–19), 1961–1973.

Environmental Mining Council of British Columbia (1996) Acid Mine Drainage. Mining and Water Pollution Issues in B.C.; B.C. Wild and the Environmental Mining Council of British Columbia: Canada, pp. (1–6)

Förstner, U.; Wittmann, G. T. W. (1998) *Metal Pollution in the Aquatic Environment*; Springer-Verlag: Berlin.

Grande, J. A.; Borrego, J.; Morales, J. A. (2000) Study of Heavy Metal Pollution in the Tinto-Odiel Estuary in Southwestern Spain Using Spatial Factor Analysis. *Environ. Geol.*, **39**(10), 1095–1101)

Grande, J. A.; Borrego, J.; Morales, J. A.; de la Torre, M. L. (2003a) A Description of How Metal Pollution Occurs in the Tinto-Odiel Rias (Huelva-Spain) through the Application of Cluster Analysis. *Mar. Pollut. Bull.*, **46,** 475–480.

Grande, J. A.; Borrego, J.; de la Torre, M. L.; Sáinz, A. (2003b) Application of Cluster Analysis to the Geochemistry Zonation of the Estuary Waters in the Tinto and Odiel Rivers (Huelva, Spain). *Environ. Geochem. Health*, **25,** 233–246.

Grande, J. A.; Beltrán, R.; Sáinz, A.; Santos, J. C.; de la Torre, M. L.; Borrego, J. (2005a) Acid Mine Drainage and Acid Rock Drainage Processes in the Environment of Herrerías Mine (Iberian Pyrite Belt, Huelva-Spain) and Impact on the Andevalo Dam. *Environ. Geol.*, **47,** 185–196.

Grande, J. A.; Andújar, J. M.; Aroba, J.; de la Torre, M. L.; Beltrán, R. (2005b) Precipitation, pH and Metal Load in AMD River Basins: An Application of Fuzzy Clustering Algorithms to the Process Characterization. *J. Environ. Monit.*, **7**(4),325–334.

Grande, J. A.; de la Torre, M. L.; Cerón, J. C.; Beltrán, R.; Gómez, T. (2010a) Overall Hydrochemical Characterization of the Iberian Pyrite Belt. Main Acid Mine Drainage-Generating Sources (Huelva, SW Spain). *J. Hydrol.*, **390,** 123–130.

Grande, J. A.; Andújar, J. M.; Aroba, J.; Beltrán, R.; de la Torre, M. L.; Cerón, J. C.; Gómez, T. (2010b) Fuzzy Modelling of the Spatial Evolution of the Chemistry in the Tinto river (SW Spain). *Water Res. Manage.*, **24,** 3219–3235.

Grande, J. A.; Andújar, J. M.; Aroba, J.; de la Torre, M. L. (2010c) Presence of As in the Fluvial Network due to AMD Processes in the Riotinto Mining Area (SW Spain): A Fuzzy Logic Qualitative Model. *J. Hazard. Mater.*, **176** (1–3), 395–401.

Grande, J. A.; Jiménez, A.; Romero, S.; de la Torre, M. L.; Gómez, T. (2010d) Quantification of Heavy Metals from AMD Discharged into a Public Water Supply Dam in the Iberian Pyrite Belt (SW Spain) Using Centered Moving Average. *Water, Air, Soil Pollut.*, **212,** 299–307.

Grande, J. A.; Jiménez, A.; Borrego, J.; de la Torre, M. L.; Gómez, T. (2010e) Relationships Between Conductivity and pH in Channels Exposed to Acid Mine Drainage Processes: Study of a Large Mass of Data Using Classical Statistics. *Water Res. Manage*., **24,** 4579–4587.

Grande, J. A. (2011) Impact of AMD Processes on the Public Water Supply: Hydrochemical Variations and Application of a Classification Model to a River in the Iberian Pyritic Belt. S.W. Spain. *Hydrol. Res*., **42**(6), 472–478.

Grande, J. A.; Aroba, J.; Andujar, J. M.; Gómez, T.; de la Torre, M. L.; Borrego, J.; Romero, S.; Barranco, C.; Santisteban, M. (2011a) Tinto Versus Odiel: Two AMD Polluted Rivers and an Unresolved Issue. An Artificial Intelligence Approach. *Water Res. Manage*., **25,** 3575-3594.

Grande, J. A.; de la Torre, M. L.; Cerón, J. C.; Sánchez-Rodas, D.; Beltrán, R. (2011b) Arsenic Speciation in the Riotinto Mining Area (SW Spain) During a Hydrological Year. *Water Practice and Technology*, **6**(1) 10.2166/wpt.2011.011

Jiménez, A.; Aroba, J.; de la Torre, M. L.; Andujar, J. M.; Grande, J. A. (2009) Model of Behaviour of Conductivity Versus pH in A.M.D. Water Bases on Fuzzy Logic and Data Mining Techniques. *J. Hydroinf*., **11** (2), 147–153.

Lake, P. A. (1991) *The Biostratigraphy and Structure of the Pulo do Lobo Domain and Iberian Pyrite Belt Domain within the Huelva Province*. Unpubl. PhD thesis, University of Southampton, pp 324.

Leblanc. M.; Morales, J. M.; Borrego. J.; Elbaz-Poulichet, F. (2000) 4.500 Year-Old Mining Pollution in Southwestern Spain: Long-Term Implications for Modern Mining Pollution. *Econ. Geol*., **95,** 655–662.

López-Pamo, E.; Sánchez España, J.; Díez Ercilla, M.; Santofimia Pastor, E.; Réyes Andrés, J. (2009) *Cortas Mineras Inundadas de la Faja Pirítica Ibérica: Inventario e Hidroquímica*; Instituto Geológico y Minero de España. Serie: Medio Ambiente. Número, 13.

Nebel, B. J.; Wright, R. T. (1999) *Ciencias Ambientales. Ecología y Desarrollo Sostenible*; Prentice Hall: México.

Nicholson, R. V. (1994) Iron-Sulfite Oxidation Mechanism. In *Chemical Weathering Rates of Silicate Minerals*; White A.F., Brantley R.J., Eds; Mineralogical Society of America; Mineralogy **31,** 173–225.

Nordstrom, D. K.; Alpers, C. N.; Coston, J. A.; Taylor, H. E.; McCleskey, R. B.; Ball, J. W.; Ogle, S.; Cotsifas, J. S.; Davis, J. A. (1999) Geochemistry, Toxicity, and Sorption Properties of Contaminated Sediments and Pore Waters from Two Reservoirs Receiving Acid Mine Drainage. In *U.S. Geological Survey Toxic Substances Hydrology Program*, Proceedings of the Technical Meeting, Charleston, South Carolina, March 8–12, 1999; Volume 1, Contamination From Hard-Rock Mining, Water-Resources Investigation Report 99-4018A.

McGillavry, H. J. (1961) The Upper Paleozoic of the Baixo Alentejo, Southern Portugal. *Econ. Geol*., **72,** 527–548.

Moreno, C. (1993). Postvolcanic Palaeozoic of the Iberian Pyrite Belt: An Example of Basin Morphologic Control on Sediment in a Turbidite Basin. *J. Sediment. Petrol.,* **63,** 1118–28.

Moreno, C.; González, F.; Sáez, R.; Sierra, S. (2003) Inicio del Vulcanismo en el Sector de Calañas (Faja Pirítica Ibérica) Caracterización y Datación. *Geogaceta*, **33,** 59–62.

Moreno, C.; González, F. (2004) Estratigrafía de la Zona Surportuguesa. In *Geología de España,* Vera, J.A., Ed.; SGE-IGME: Madrid, pp. 201–205.

Moreno, C.; Sáez, R. (1990) Sedimentación Marina Somera en el Anticlinorio de Puebla de Guzmán. *Geogaceta*, **8,** 62–64.

Oliveira, J. T. (1983). The Marine Carboniferous of South Portugal. A Stratigraphic and Sedimentological Approach. *Mem. Servo Geol. Port.,* **29,** 3–37.

Pinedo Vara, I. (1963) *Piritas de Huelva*; Madrid, Summa.

Sáez, R.; Moreno, C. (1997) Geology of the Puebla de Guzmán Anticlinorium. In *Geology and VMS Deposits of the Iberian Pyrite Belt;* de Sousa Barriga, F. J. A.; de Carvalho, D); Society of Economic Geologists Guidebook Series 27: Littleton (Colorado); 131–136.

Sáez, R.; Pascual, E.; Toscano, M.; Almodovar, G. (1999) The Iberian Type of Volcano-Sedimentary Massive Sulphide Deposits. *Miner. Deposita*, **34,** 549–570

Sáez, R.; Moreno, C.; González, F.; Almodóvar, G. (2011) Black Shales and Massive Sulfides: Causal or Casual Relationships? Insights from Rammelsberg, Tharsis, and Draa Sfar. *Miner. Deposita*, 46 (5–6), 585–614.

Sáinz, A. (1999) *Estudio de la Contaminación Química de Origen Minero en el Río Odiel*. PhD Thesis. University of Huelva.

Sáinz, A.; Grande, J. A.; de la Torre, M. L.; Sánchez-Rodas, D. (2002) Characterisation of Sequential Leachate Discharges of Mining Waste Rock Dumps in the Tinto and Odiel Rivers. *J. Environ. Manage*., **64** (4)**,** 345–353.

Sáinz, A.; Grande, J. A.; de la Torre, M. L. (2003a) Analysis of the Impact of Local Corrective Measures on the Input of Contaminants from the Odiel River to the Ria of Huelva (Spain). *Water, Air, Soil Pollut*., **144,** 375–389.

Sáinz, A.; Grande, J. A.; de la Torre, M. L. (2003b) Odiel River, Acid Mine Drainage and Current Characterisation by Means of Univariate Analysis. *Environ. Int*., **29,** 51–59.

Sáinz A.; Grande, J. A.; de la Torre, M. L. (2004) Characterization of Heavy Metal Discharge into the Ria of Huelva. *Environ. Int*., **30,** 557–566.

Sainz, A.; Grande, J. A.; de la Torre, M. L. (2005) Application of a Systemic Approach to the Study of Pollution of the Tinto and Odiel rivers (Spain). *Environ. Monit. Assess*., **102,** 435–445.

Sanchez-España, J.; Velasco, F.; Yusta, I. (2000) Hydrothermal Alteration of Felsic Volcanic Rocks Associated with Massive Sulphide Deposition in the Northern Iberian Pyrite Belt (SW Spain). *Appl. Geochem*., **15** (9), 1265–1290.

Santofimia, E.; López-Pamo, E.; Reyes, J. (2012) Changes in Stratification and Iron Redox Cycle of an Acidic Pit Lake in Relation with Climatic Factors and Physical Processes. *J. Geochem. Explor*., **116–117,** 40–50.

Sarmiento, A. M.; Olías, M.; Nieto, J. M.; Cánovas, C. R.; Delgado, J. (2009) Natural Attenuation Processes in Two Water Reservoirs Receiving Acid Mine Drainage. *Sci. Total Environ*., **407,** 2051–2062.

Schlesinger, W. H. (2005) *Biogeochemistry. Treatise on Geochemistry, Volume* 8; Elsevier Science: Oxford, pp. 720.

Tornos, F.; Heinrich, C. A. (2008) Shale Basins, Sulphur-Deficient Ore Brines, and the Formation of Exhalative Base Metal Deposits. *Chem. Geol*., **247,** 195–207.

Torres, E.; Ayora, C.; Ruiz, C.; Sarmiento, A. M. (2010) Geochemical Controls of Two Water Reservoirs That Receive Acid Mine Drainage in the Odiel Basin. *Revista de la Sociedad Española de Mineralogía*, **13,** 215.

Valente, T.; Leal Gomes, C. (2009) Occurrence, Properties and Pollution Potential of Environmental Minerals in Acid Mine Drainage. *Sci. Total Environ*., **407,** 1135–1152.

Vasquez, O.; Monnell, J. D.; Pu, X.; Neufeld, D. (2011) Major Processes Dominating the Release of Aluminum from Smectite Clays When Leached With Acid Mine Drainage. *Environ. Eng. Sci*., **28,** 163–169.

Wetzel, D. B. (2001) *Limnology: Lake and River Ecosystems*, 3rd Edition; Academic Press: San Diego, p. 1006.

Younger, P. L. (2002) Coalfield Closure and the Water Environment in Europe. *Transactions of the Institution of Mining and Metallurgy (Section A: Mining Technology),* **111,** 201–209.

Yusta, I.; Martínez, A.; Velasco, F. (2002) Litogeoquímica de las Pizarras Negras de la Faja Pirítica Ibérica: Implicaciones en la Génesis de los Sulfuros Masivos. *Boletín de la Sociedad Española de Mineralogía*, **25A,** 107–108.